Structural and Chemical Characterization of Aligned Crystalline Nanoporous MgO Films Grown via Reactive Ballistic Deposition

Z. Dohnálek, Greg A. Kimmel, David E. McCready, James S. Young, Alice Dohnálková, R. Scott Smith, and Bruce D. Kay*

Pacific Northwest National Laboratory, W. R. Wiley Environmental Molecular Sciences Laboratory, P.O. Box 999, MSN K8-88, Richland, Washington 99352

Received: October 15, 2001; In Final Form: December 17, 2001

Highly porous (∼ 90%), high-surface area (∼1000 m^2/g), thermally stable (1200 K) crystalline films of MgO are synthesized using a novel reactive ballistic deposition technique. The film consists of a tilted array of porous nanoscale crystalline filaments. Surprisingly, the individual filaments exhibit a high degree of crystallographic order with respect to each other. These films have chemical binding sites analogous to those on MgO(100). However, the fraction of chemically active, high energy binding sites is greatly enhanced on the nanoporous film. This unique collection of properties makes these materials attractive candidates for chemical applications such as sensors and heterogeneous catalysts.

The novel properties of supported nanocrystalline materials and their potential use in a variety of technologies are currently driving research efforts in a number of physical sciences. The ultimate goal is to tune the physical and/or chemical properties of these materials by controlling their structure on a nanometer scale. A number of different approaches[1−5] including ballistic deposition[6,7] have been employed to grow a wide range of porous thin film materials with interesting structural,[1−3,6,7] chemical,[4,5] optical,[8] electronic,[9] and magnetic properties.[10,11] Despite their exciting physical properties, there are no prior studies related to the chemical activity of nanoporous films grown via ballistic deposition. In this report we present the first synthesis and characterization (structural and chemical) of nanoporous crystalline MgO, a catalytically relevant material grown via reactive ballistic deposition.

Nanoporous MgO films having surface areas of ∼1000 m^2/g were synthesized using a novel reactive ballistic deposition technique. These films are comprised of a tethered array of individual filaments characteristic of films grown at glancing angles of deposition.[12,13] Surprisingly, we find that these individual filaments are crystalline with very high internal surface areas. Furthermore, the crystalline axes of the individual filaments are aligned relative to each other leading to a highly "textured" nanoporous film. Chemically, we find adsorbate binding sites within the porous films which are analogous to those observed on monocrystalline MgO(100) surfaces allowing for the direct comparison of the sites. However, the number of chemically active "defect" sites such as steps and kinks is greatly increased for the porous films. This is in agreement with the enhanced chemical activity of high surface area (∼500 m^2/g) MgO nanocrystals recently synthesized and characterized by Klabunde and co-workers.[4,5] Importantly, the population of the various sites can be controlled by tuning the ballistic deposition growth conditions.

To grow porous thin films of MgO, we employ a new ballistic deposition (BD) technique, which we refer to as reactive ballistic deposition (RBD). In RBD, the final compound is formed on the surface of the film by the reaction of a directed beam of one of the reactants with a nondirectional source (e.g. ambient gas) of the second reactant. For the studies reported herein a collimated atomic beam of Mg is deposited at glancing angle of incidence on the growing film in a background pressure of O_2. Since RBD uses independent sources for the reacting species it is, in principle, possible to control both the composition and the structure of the film. The compositional control of the film is analogous to that obtained using molecular beam epitaxy in a reactive gas ambient.[14] Due to the simple physical principles underlying the RBD technique, we believe that it can be used for the growth of a broad range of chemically tailored, nanoporous materials.

Nanoporous MgO films were grown on several substrates including oxidized Si(100) and Si(111), fused silica, and atomically clean Mo(100). Although we have studied film growth as a function of deposition angle and growth temperature, the films presented in this report were grown in the temperature range of 200−300 K with a Mg beam deposition angle of 85° (with respect to normal) in an oxygen rich environment (pressure of 1×10^{-6}−1×10^{-5} Torr). The optical properties of the growing films were monitored using laser interferometry.[15] The index of refraction of dense MgO deposited at normal angle of incidence was measured to be 1.75 ± 0.03 at 632.8 nm in good agreement with tabulated value of 1.735.[16] Growth at 85° resulted in porous films with an index of refraction of 1.06 ± 0.02 corresponding to a porosity of ∼90% according to the Lorentz−Lorenz relationship.[17] Structural characterization of the films included ex situ analysis using scanning electron microscopy (SEM), high-resolution transmission electron microscopy (HRTEM), and X-ray diffraction (XRD). Collectively these techniques show that the films are crystalline MgO.

Surface area measurements and chemical characterization of the films were performed in situ primarily by N_2 adsorption/desorption studies.[7,18,19] Since Mo(100) can be used as a substrate for the epitaxial growth of dense, atomically flat, MgO-(100) films,[20,21] the physisorption studies were performed on nanoporous films grown on this substrate. This facilitated direct comparison of adsorption sites present on nanoporous MgO

* To whom correspondence should be addressed.

10.1021/jp013801c CCC: $22.00 © 2002 American Chemical Society
Published on Web 02/12/2002

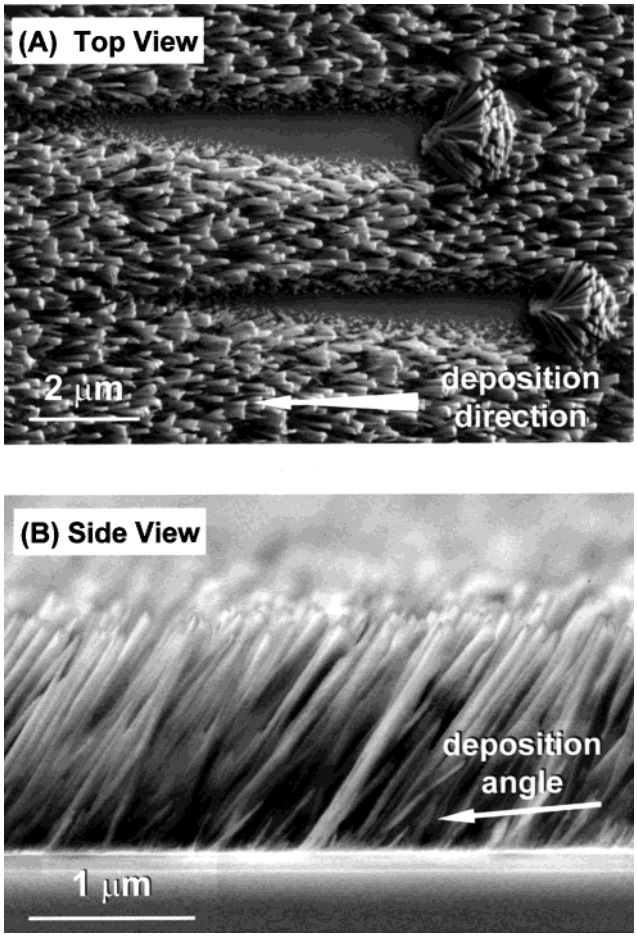

Figure 1. SEM images of a 1.5 μm thick, nanoporous MgO film grown on oxidized Si(111) at room temperature and deposition angle of 85°. (A) Top view. Two dust particles illustrate the shadowing of the incident deposition flux. (B) Side view. The filaments are tilted away from the surface normal toward the direction of the incident Mg beam at an angle of ~30° with a fwhm of 15°.

films with those of single-crystal MgO(100). The N_2 was adsorbed under conditions that prevent multilayer formation on a flat MgO(100) surface. The N_2 physisorbed on the film was subsequently desorbed by applying a linear temperature ramp and the desorbed molecules were detected with a quadrupole mass spectrometer. The N_2 physisorption studies were performed on films which were significantly thinner (~100 nm) than those examined with SEM, HRTEM, and XRD.

Figure 1 shows top (Figure 1a) and side-view (Figure 1b) SEM micrographs of a 1.5 μm thick porous MgO film grown on Si(111) at room temperature. The film is composed of filaments that are tilted 30° off-normal toward the incident Mg beam. In agreement with previous studies the filament tilt angle is smaller that the incident angle of the growth beam.[19,22]

In Figure 1a, two dust particles initially present on the substrate nicely illustrate the shadowing effect (albeit on a larger scale) responsible for porous growth under BD conditions. BD occurs when surface diffusion is slow compared to the rate at which particles arrive from the gas phase.[6,22] In that case the impinging particles are incorporated directly at, or in very close proximity to, their original landing site. The inherent randomness of the deposition process results in the formation of atomic scale asperities on the surface, which preferentially capture incoming flux. In a manner analogous to the dust particles, these asperities provide the attachment points and shadowing necessary for the filamentous growth. As evident from Figure 1, there is no long-range translational periodicity between the individual filaments. When smaller deposition angles are employed (data not shown) the average filament-filament separation decreases. For incident angles smaller than ~70° the filament-like structure disappears in agreement with previous measurements.[12,13]

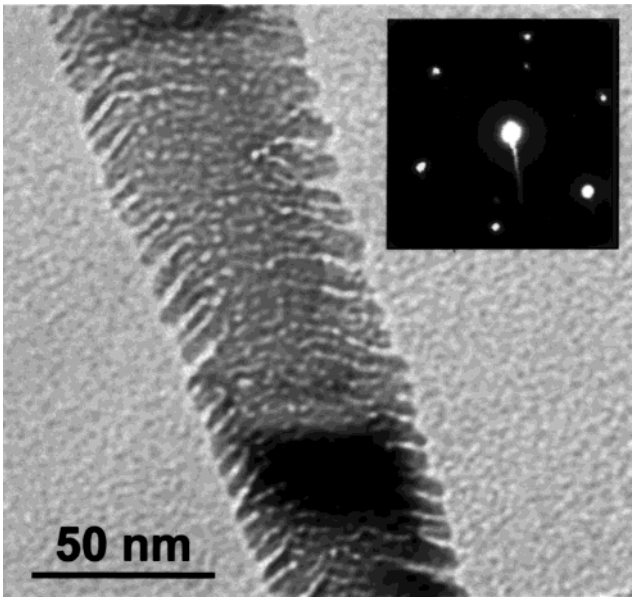

Figure 2. HRTEM image of an MgO filament. The image reveals the feather-like internal pore structure typical of filaments from the film shown in Figure 1. A selected area diffraction pattern demonstrating the crystalline nature of the filament is shown in the inset.

Numerous previous studies have used SEM to image the morphology of porous films grown via BD.[8,12,13] At resolutions typical for SEM images, the individual filaments appear dense and relatively smooth as evident from Figure 1. We have also focused on exploring the structure of individual MgO filaments using HRTEM. The analysis was performed on filaments that were collected from the growth substrate and placed on a standard Formvar coated copper grid. Typical filament structure is shown in Figure 2. Remarkably, the individual filaments are highly porous but have a regular overall shape suggestive of a nanocrystallite. The crystalline nature of the individual filament is confirmed by selected area diffraction as shown in the insert in Figure 2. The feather-like structure of the individual filaments indicates that porous MgO has a very high surface area desirable for possible chemical applications. To the best of our knowledge this is the first report that examines the nanostructure of the individual filaments.

Selected area diffraction reveals that the individual filaments are crystalline. However, given the apparent disorder evident in the SEM images (Figure 1) the relative crystallographic orientation of individual filaments is uncertain. To address this issue we have used X-ray diffraction. These diffraction experiments show that the orientations of the crystalline filaments are highly aligned with respect to each other, i.e., the films are highly "textured".[23] Furthermore, the orientation of the textured film is dependent on the substrate. Figure 3 shows the results of an X-ray texture analysis of roughly 1 μm thick nanoporous MgO films grown on oxidized Si(111) (Figure 3a,c) and atomically clean Mo(100) (Figure 3b,d) deposited at 300 K. The distribution of {200} pole intensities are plotted as stereographic projections in Figure 3a,b. The diffraction patterns indicate that the filaments are aligned with respect to the surface normal and azimuthally aligned with respect to each other. As evident from the comparison of Figure 3a and Figure 3b, the crystallographic orientation of these two films is different. The

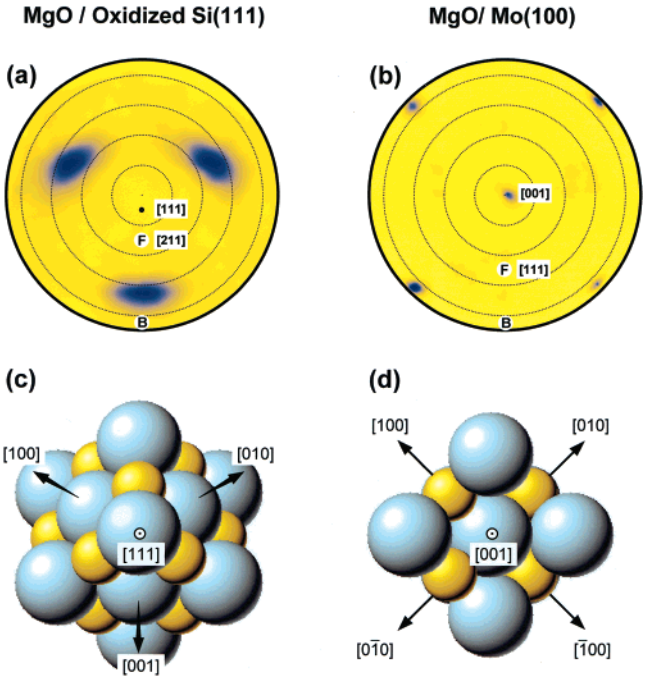

Figure 3. X-ray diffraction {200} pole figures of MgO films deposited at room temperature and deposition angle of 85° on (a) oxidized Si-(111) and (b) atomically clean Mo(100). The well-resolved intensity maxima indicate a high level of crystallographic alignment ("texture") of the individual filaments with respect to the substrate. The directions of the incident Mg beam and the long axes of filaments are labeled B and F, respectively. The corresponding orientations of the MgO unit cells (Mg, blue; O, yellow) with respect to the substrate (plane of paper) are shown in (c) and (d).

crystallographic orientation of the rock salt unit cells for the diffraction patterns displayed in Figures 3a and 3b is shown in Figures 3c and 3d, respectively. The full width at half-maximum (fwhm) of the {200} poles in Figure 3a is ∼15° which is consistent with the distribution of filament tilt angles shown in Figure 1b. The SEM and XRD data indicate that the long axes of the filaments are preferentially aligned along [211] and [111] MgO crystallographic directions for films grown on Si(111) and Mo(100) substrates, respectively.

Since MgO grows epitaxially on Mo(100), the crystallographic orientation of the film is determined by the orientation of the substrate. The observed texture in Figure 3b is consistent with this explanation. For films grown on oxidized silicon and fused silica substrates, MgO does not grow epitaxially. Therefore the origin of the texture observed in Figure 3a is not fully understood. A possible explanation could be "evolutionary selection" as outlined by van der Drift[24] for the growth of dense, textured, polycrystalline films. In this scenario, as a film grows, the grains in the film which grow the fastest will prevail. Hence, even if nucleation is random, filaments with the preferred orientation will grow the fastest and will eventually shadow the slower growing filaments.

From the SEM (Figure 1) and HRTEM (Figure 2) images, the MgO films grown via RBD have a somewhat regular structure composed of individual crystalline filaments, which have high internal surface areas. These properties of nanoporous films, as demonstrated in this specific case for MgO, make them good candidates for chemical applications. As a first step in the chemical characterization, we have studied the physisorption of N_2 by the nanoporous MgO films. In general, physisorption is a very sensitive probe of the interaction between the substrate and the adsorbate and is thus a good probe of the distribution of binding sites[21] on the surface where the relevant chemistry will occur. Physisorption also allows us to measure the adsorption capacity of the porous films, i.e., to measure the total number of adsorption sites.[7,18] The surface area information obtained is analogous to that from N_2 Brunauer−Emmett−Teller (BET) isotherm measurements.[25]

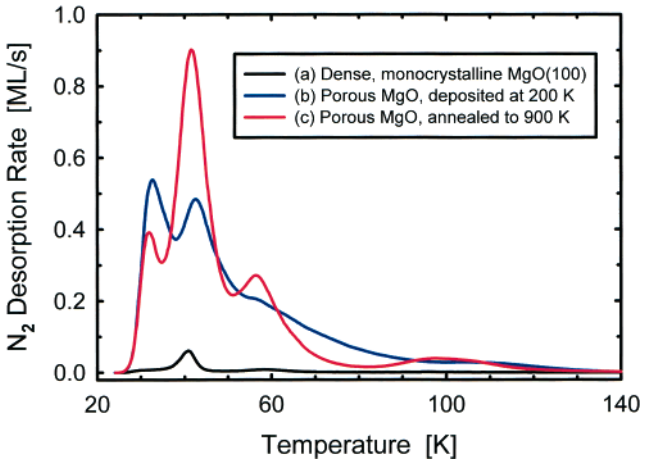

Figure 4. Temperature programmed desorption spectra of N_2 physisorbed on thin MgO films. All films contain an equal amount of MgO equivalent to 40 layers of dense MgO(100). (a) N_2 TPD (black spectrum) from dense monocrystalline MgO(100). (b) N_2 TPD (blue spectrum) from nanoporous MgO grown at 200 K and 85°. (c) N_2 TPD (red spectrum) obtained after annealing film (b) to 900 K.

Temperature programmed desorption (TPD) spectra for N_2 on a dense monocrystalline MgO(100) film (black line), a nanoporous MgO deposited at 200 K (blue), and the same nanoporous MgO film after annealing to 900 K (red) are shown in Figure 4. The N_2 TPD from the dense monocrystalline MgO-(100) surface is dominated by a single desorption feature at 42 K which corresponds to the desorption of N_2 from MgO(100) terraces. The temperature at which the desorption is observed is determined by the strength of the interaction between the adsorbate and the substrate. A small amount of desorption at higher temperatures (48−80 K) is also observed and is associated with desorption from morphological defects such as steps and kinks. The area under the curve represents a single layer of N_2 adsorbed on an atomically flat MgO(100) surface and corresponds to 7.8×10^{14} N_2/cm^2.[26]

For the porous films used in the TPD studies, the amount of material is equivalent to 40 atomic layers of dense MgO(100). However, since the porosity of these films is ∼90% (as measured by optical interference), these films have a mean thickness of ∼400 layers. In contrast to the dense MgO(100) film, the N_2 desorption from a nanoporous MgO film grown at 200 K (blue line) occurs over a very broad temperature range (25−140 K), indicating a wide range of binding sites. As expected for a porous film, a dramatic increase of the amount of adsorbed N_2 is observed. The area under the entire curve is ∼27 times greater than that of the dense film and represents roughly 1 N_2 adsorbed per 2 MgO units. This level of adsorption corresponds to a specific surface area of ∼1000 m^2/g.[27]

After annealing to 900 K, the nanoporous film retains its high surface area as shown in Figure 4 (red line). However, the N_2 TPD line shape, which was previously broad and unresolved, displays a series of four relatively well-defined peaks at ∼32, 42, 56, and 98 K. The peaks at 42 and 56 K are also observed on the dense MgO(100) and correspond to N_2 desorption from the MgO(100) terraces and defects, respectively. The N_2 desorption feature at 98 K is due to adsorption at a much stronger binding site which is not observed on the dense MgO-

(100). The intensity of the low temperature feature at 32 K is extremely sensitive to the N_2 dose temperature and is most likely the result of N_2 condensed within the nanopores of individual filaments.[7,18,19] This low-temperature adsorption contributes only about 16% to the calculated surface area.

The changes in the TPD spectra upon annealing are suggestive of enhanced ordering of the crystalline film due to short-range diffusive motion. This interpretation is also supported by low-energy electron diffraction (LEED) (data not shown), a technique sensitive to surface order. This ordering results in an increase in the fraction of terrace sites observed in the N_2 TPD (42 K peak). Repeated annealings produce no further changes in the film, as characterized by N_2 TPD and LEED. Although not shown here, the films begin to densify at 1200 K and become fully dense by 1400 K.

The nanoporous MgO films have high surface areas and porosities. However, the origin of these two properties are quite different. In the SEM images (Figure 1) the filaments appear smooth and dense leading to a calculated surface area of ~20 m^2/g. However, the actual surface area as measured with N_2 adsorption is about 50-fold greater and arises from the intra-filament, feather-like nanostructure observed via HRTEM (Figure 2). The HRTEM images also reveal that the density of the individual filaments is relatively high and hence the high film porosity (observed by optical interference measurements) arises predominantly from the relatively large inter-filament spacing observed with SEM. These characteristics should be advantageous for catalytic materials since large interfilament spacing will facilitate reactant and product transport to and from the intrafilament sites. This is supported by additional experiments (not shown) where we find that N_2 uptake into the nanoporous MgO film occurs with near unit probability and preferentially finds the strongest binding sites.

As we have demonstrated above, the RBD technique can be used to synthesize extremely porous (90%), high surface area (1000 m^2/g), thermally robust (1200 K), nanoporous, highly textured, crystalline MgO films. The surface areas of these films exceed those of traditionally prepared MgO powders (2−100 m^2/g)[28] and nanocrystals (400−500 m^2/g).[4,5] Due to the physical simplicity of the RBD technique we anticipate that it should be applicable to the synthesis of a broad range of chemically tailored, catalytically active materials. For example, using multiple beams it should be possible to decorate the nanoporous oxide support with catalytically active metals. We are actively engaged in the synthesis and chemical characterization of these novel materials.

Acknowledgment. This work was supported by the U.S. Department of Energy Office of Basic Energy Sciences, Chemical Sciences Division and the LDRD investments from PNNL. It was performed at the W. R. Wiley Environmental Molecular Sciences Laboratory, a national scientific user facility sponsored by the Department of Energy's Office of Biological and Environmental Research and located at Pacific Northwest National Laboratory. Pacific Northwest National Laboratory is operated for the U.S. Department of Energy by Battelle under Contract DE-AC06-76RLO 1830.

References and Notes

(1) Valden, M.; Lai, X.; Goodman, D. W. *Science* **1998**, *281*, 1647.
(2) Aggarwal, S.; Monga, A. P.; Perusse, S. R.; Ramesh, R.; Ballarotto, V.; Williams, E. D.; Chalamala, B. R.; Wei, Y.; Reuss, R. H. *Science* **2000**, *287*, 2235.
(3) Bowden, N.; Brittain, S.; Evans, A. G.; Hutchinson, J. W.; Whitesides, G. M. *Nature* **1998**, *393*, 146.
(4) Richards, R.; Li, W. F.; Decker, S.; Davidson, C.; Koper, O.; Zaikovski, V.; Volodin, A.; Rieker, T.; Klabunde, K. J. *J. Am. Chem. Soc.* **2000**, *122*, 4921.
(5) Klabunde, K. J.; Stark, J.; Koper, O.; Mohs, C.; Park, D. G.; Decker, S.; Jiang, Y.; Lagadic, I.; Zhang, D. J. *J. Phys. Chem.* **1996**, *100*, 12142.
(6) Barabási, A. L.; Stanley, H. E. *Fractal Concepts in Surface Growth*; Cambridge University Press: Cambridge, 1995.
(7) Stevenson, K. P.; Kimmel, G. A.; Dohnálek, Z.; Smith, R. S.; Kay, B. D. *Science* **1999**, *283*, 1505.
(8) Robbie, K.; Brett, M. J.; Lakhtakia, A. *Nature* **1996**, *384*, 616.
(9) Venugopal, V. C.; Lakhtakia, A.; Messier, R.; Kucera, J. P. *J. Vac. Sci. Technol. B* **2000**, *18*, 32.
(10) Smith, D. O.; Cohen, M. S.; Weiss, G. P. *J. Appl. Phys.* **1960**, *31*, 1755.
(11) Bijker, M. D.; Visser, E. M.; Lodder, J. C. *Tribol. Int.* **1998**, *31*, 553.
(12) Robbie, K.; Brett, M. J. *J. Vac. Sci. Technol., A* **1997**, *15*, 1460.
(13) Sit, J. C.; Vick, D.; Robbie, K.; Brett, M. J. *J. Mater. Res.* **1999**, *14*, 1197.
(14) Chambers, S. A. *Surf. Sci. Rep.* **2000**, *39*, 105.
(15) Heavens, O. S. *Optical Properties of Thin Solid Films*; Dover Publications: New York, 1991.
(16) Stephens, R. E.; Malitson, I. H. *J. Res. NBS* **1952**, *49*, 249.
(17) Born, M.; Wolf, E. *Principles of Optics*; Pergamon: Oxford, 1975.
(18) Kimmel, G. A.; Stevenson, K. P.; Dohnalek, Z.; Smith, R. S.; Kay, B. D. *J. Chem. Phys.* **2001**, *114*, 5284.
(19) Kimmel, G. A.; Dohnalek, Z.; Stevenson, K. P.; Smith, R. S.; Kay, B. D. *J. Chem. Phys.* **2001**, *114*, 5295.
(20) Wu, M.-C.; Corneille, J. S.; Estrada, C. A.; He, J.-W.; Goodman, D. W. *Chem. Phys. Lett.* **1991**, *182*, 472.
(21) Dohnálek, Z.; Kimmel, G. A.; Joyce, S. A.; Ayotte, P.; Smith, R. S.; Kay, B. D. *J. Phys. Chem. B.* **2001**, *105*, 3747.
(22) Abelmann, L.; Lodder, C. *Thin Solid Films* **1997**, *305*, 1.
(23) Wenk, H.-R. *Preferred Orientation in Deformed Metals and Rocks: An Introduction to Modern Texture Analysis*; Academic Press: Orlando, 1985.
(24) van der Drift, A. *Philips Res. Rep.* **1967**, *22*, 267.
(25) Gregg, S. J.; Sing, K. S. W. *Adsorption, Surface Area, and Porosity*, 2nd ed.; Academic Press: London, 1982.
(26) Trabelsi, M.; Coulomb, J. P.; Degenhardt, D.; Lauter, H. *Surf. Sci.* **1997**, *377*, 38.
(27) The specific surface area of the nanoporous MgO film is defined to be the ratio of the surface area of adsorbed N_2 to the mass of MgO in the film. The N_2 surface area is defined as the product of the number of N_2 monolayers adsorbed and the area of the incident N_2 beam. The mass of MgO exposed to the N_2 beam is the product of the area of the N_2 beam (~0.3 cm^2), the number of equivalent layers of dense MgO in the film (40 ML), the height per MgO monolayer (2.1 Å/ML), and the bulk MgO density (3.6 g/cm^3). (The saturated monolayer of N_2 on dense MgO(100) is assumed to have the geometric area of the N_2 beam.).
(28) Larese, J. Z. *Physica B* **1998**, *248*, 297.